



# Crystal structure of a small heat-shock protein from *Xylella fastidiosa* reveals a distinct high-order structure

Emanuella Maria Barreto Fonseca,<sup>a,‡</sup> Valéria Scorsato,<sup>a</sup> Marcelo Leite dos Santos,<sup>a,§</sup> Atilio Tomazini Júnior,<sup>b</sup> Susely Ferraz Siqueira Tada,<sup>c</sup> Clelton Aparecido dos Santos,<sup>c</sup> Marcelo Augusto Szymanski de Toledo,<sup>c</sup> Anete Pereira de Souza,<sup>c</sup> Igor Polikarpov<sup>b</sup> and Ricardo Aparicio<sup>a</sup>

Received 5 December 2016

Accepted 14 March 2017

Edited by I. Tanaka, Hokkaido University, Japan

‡ Current address: Federal Institute of Education, Science and Technology of Sao Paulo (IFSP), Campus São Roque, Rodovia Prefeito Quintino de Lima 2100, 18136-540 São Roque-SP, Brazil.

§ Current address: Department of Chemistry (DQCI), Universidade Federal de Sergipe (UFS), Campus Professor Alberto Carvalho, Avenida Vereador Olimpio Grande s/n, 49500-000 Itabaiana-SE, Brazil.

**Keywords:** small heat-shock protein; *Xylella fastidiosa*;  $\alpha$ -crystallin domain; citrus variegated chlorosis; XfsHSP17.9; chaperones.

**PDB reference:** small heat-shock protein from *X. fastidiosa*, 5j7n

**Supporting information:** this article has supporting information at journals.iucr.org/f

<sup>a</sup>Laboratory of Structural Biology and Crystallography, Institute of Chemistry, University of Campinas, CP6154, 13083-970 Campinas-SP, Brazil, <sup>b</sup>Molecular Biotechnology Group, Department of Physics and Interdisciplinary Science, Sao Carlos Institute of Physics (IFSC), University of Sao Paulo (USP), Avenida Trabalhador São-carlense 400, Parque Arnold Schmidt, 13566-590 São Carlos-SP, Brazil, and <sup>c</sup>Laboratory of Molecular and Genetic Analysis, Center for Molecular Biology and Genetic Engineering, Institute of Biology, University of Campinas, CP6010, 13083-875 Campinas-SP, Brazil

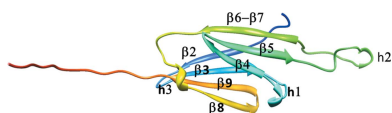
Citrus variegated chlorosis is a disease that attacks economically important citrus plantations and is caused by the plant-pathogenic bacterium *Xylella fastidiosa*. In this work, the structure of a small heat-shock protein from *X. fastidiosa* (XfsHSP17.9) is reported. The high-order structures of small heat-shock proteins from other organisms are arranged in the forms of double-disc, hollow-sphere or spherical assemblies. Unexpectedly, the structure reported here reveals a high-order architecture forming a nearly square cavity.

## 1. Introduction

Heat-shock proteins (HSPs) are a group of proteins that are usually classified based on their molecular weights, including HSP100, HSP90, HSP70, HSP60 and small HSPs (sHSPs) (Trent, 1996). Many of these proteins work as chaperones, catalyzing the refolding of denatured proteins, assuring the correct fold of newly synthesized proteins and preventing protein aggregation (Laksanalamai & Robb, 2004).

sHSPs comprise the most widespread but also the least conserved family of molecular chaperones. Phylogenetic analyses suggest that sHSPs diverged early in evolution (Kappé *et al.*, 2002; Waters *et al.*, 1996), and sHSP family members have been found in all kingdoms of life (Takeda *et al.*, 2011). Bacteria (except rhizobia), archaea and unicellular eukaryotes usually contain at least one or two sHSPs (Laksanalamai & Robb, 2004; Kappé *et al.*, 2002; Allen *et al.*, 1992; Horwitz, 1992). Additionally, sHSPs are ATP-independent 'holdase' proteins, which can prevent the aggregation of partially folded proteins, stabilizing them and presenting client proteins to foldases (ATP-driven chaperones; Slepnev & Witt, 2002).

Although the proteins belonging to this superfamily are different in sequence and size, they share several important molecular features, including (i) a conserved  $\alpha$ -crystallin domain containing up to 80 amino-acid residues, (ii) a low molecular weight (12–43 kDa), (iii) the formation of large oligomers, (iv) a dynamic quaternary structure and (v) induction under stress conditions and a chaperone activity which suppresses the aggregation of proteins (Laksanalamai & Robb, 2004; Kappé *et al.*, 2002; Haslbeck *et al.*, 2005; de Jong *et al.*, 1998).



While a number of sHSPs have been identified over the past decades, their function remained unknown until *in vitro* studies in the early 1990s demonstrated that sHSPs bind to denatured proteins and prevent irreversible aggregation. Bovine  $\alpha$ -crystallin and murine HSP25 were the first sHSPs that were reported to have chaperone activity (Horwitz, 1992; Haslbeck *et al.*, 2005; Jakob *et al.*, 1993).

The mechanism of substrate recognition and interaction of sHSPs is still poorly understood (White *et al.*, 2006). It is known that sHSPs are capable of the binding and stabilization of proteins denatured by heat or other stresses in order to avoid aggregation (van Montfort *et al.*, 2001). This function is achieved by the presence of hydrophobic pockets in their structures, which are located on the surface of the molecule. Under non-stress conditions, the hydrophobic sites are protected from exposure to the solvent by the formation of oligomers containing 12–40 subunits (Saibil, 2000; Haslbeck *et al.*, 1999; Rao *et al.*, 1998; Lee *et al.*, 1997).

The large oligomer constantly changes its subunits, and dissociates into smaller oligomeric states under stress conditions. Therefore, it is believed that the hydrophobic moieties are controlled by the transition between different oligomeric states (Takeda *et al.*, 2011; de Jong *et al.*, 1998; Haslbeck *et al.*, 1999; Yang *et al.*, 1999; Shashidharamurthy *et al.*, 2005; Bova *et al.*, 2000). In fact, an increase in the exchange of subunits at high temperatures has been observed for several sHSPs, including  $\alpha$ -crystallin and human HSP27, and temperature-induced dissociation has been described for yeast HSP26 (Bova *et al.*, 2000; van den Oetelaar *et al.*, 1990; Haslbeck *et al.*, 1999).

Several structures of sHSPs have been reported: *Taenia saginata* Tsp36 (PDB entry 2bol; Stamler *et al.*, 2005), *Triticum aestivum* HSP16.9 (PDB entry 1gme; van Montfort *et al.*, 2001), *Methanococcus jannaschii* HSP16.5 (PDB entries 1shs and 4eld; Kim *et al.*, 1998; Mchaourab *et al.*, 2012), *Rattus norvegicus* HSP20 (PDB entry 2wj5; Bagn eris *et al.*, 2009), *Saccharomyces cerevisiae* HSP26.0 (PDB entries 2h50 and 2h53; White *et al.*, 2006), *Sulfolobus tokodaii* HSP14.0 (PDB entries 3vqk, 3vql, 3vqm, 3aab and 3aac; Takeda *et al.*, 2011; Hanazono *et al.*, 2012), *Xanthomonas citri* HspA (PDB entries 3gla and 3gt6; Hilario *et al.*, 2006, 2011), *Deinococcus radiodurans* HSP17.7 (PDB entry 4fei; Bepperling *et al.*, 2012), *Schizosaccharomyces pombe* HSP16.0 (PDB entry 3wlz; Hanazono *et al.*, 2013) and *Caenorhabditis elegans* HSP17.8 (PDB entries 4ydz and 4ye0; Fleckenstein *et al.*, 2015). They all feature the  $\beta$ -sandwich fold of the  $\alpha$ -crystallin domain (ACD), consisting of two antiparallel  $\beta$ -sheets composed of three and four  $\beta$ -strands.

Recently, initial crystallographic studies of an sHSP from *Xylella fastidiosa* (XfsHSP17.9) were published (Tada *et al.*, 2012). *X. fastidiosa* is the infectious agent that causes citrus variegated chlorosis (CVC). First registered in Brazil in 1987, CVC is a disease that affects many varieties of commercial citrus plants. Affected fruits are small, hardened and have no commercial value, and are responsible for significant economic losses (Simpson *et al.*, 2000; Rossetti *et al.*, 1990). Thus, efforts to prevent and to combat this infection are

needed. In this present work, we report the 2.90   resolution crystal structure of *X. fastidiosa* small heat-shock protein and reveal that it is significantly different in its high-order structure with respect to other known sHSPs.

## 2. Experimental

### 2.1. Crystallization, X-ray data collection and refinement

Azzoni and coworkers previously described the cloning, expression and purification of XfsHSP17.9 (UniProt code Q9PBB0; Azzoni *et al.*, 2004). Purified protein was submitted to crystallization experiments. X-ray data collection and processing was performed as reported by Tada *et al.* (2012).

Initial data processing revealed that the best structure solution was obtained in space group  $P4_322$ . Chain A of the *X. citri* HspA structure (PDB entry 3gla; UniProt code Q8PNC2; Hilario *et al.*, 2006, 2011) was used as a template for molecular replacement because of its high sequence similarity of 88%. The final model was obtained after reconstruction and refinement steps with *Coot* v.0.6.2 (Emsley & Cowtan, 2004)

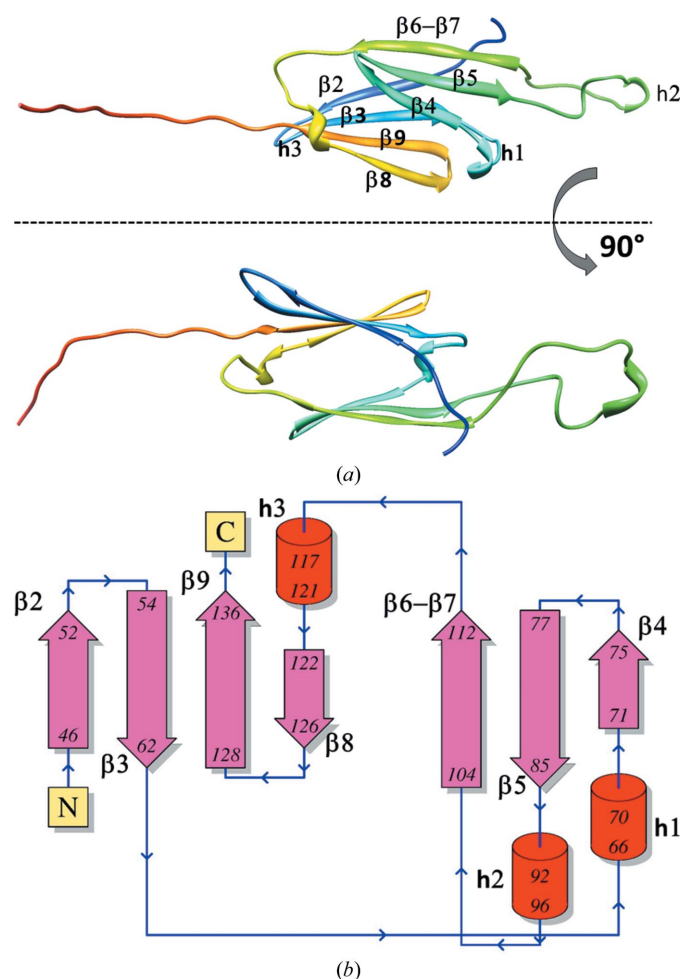


**Figure 1**  
Folding (a) and topology (b) of XfsHSP17.9. The structure consists of seven  $\beta$ -strands and three  $3_{10}$ -helices.  $\beta$ -Strands are numbered according to the convention used for *M. jannaschii* HSP16.5 (Kim *et al.*, 1998) and *X. citri* HspA (Hilario *et al.*, 2011).

**Table 1**  
X-ray data-collection and refinement statistics.

Values in parentheses are for the highest resolution shell.

PDB code	5j7n
Data-collection statistics	
Space group	<i>P</i> 4 <sub>3</sub> 22
Unit-cell parameters (Å)	<i>a</i> = <i>b</i> = 68.9, <i>c</i> = 72.5
Resolution range (Å)	40.45–2.90 (3.00–2.90)
Multiplicity	18.6 (19.3)
<i>R</i> <sub>merge</sub> (%)	11.5 (67.3)
⟨ <i>I</i> /σ( <i>I</i> )⟩	17.3 (3.5)
Refinement statistics	
Resolution (Å)	2.90
No. of reflections used	4085
Completeness (%)	97.31
No. of protein atoms	848
No. of water molecules	0
No. of reflections used for <i>R</i> <sub>free</sub> (5%)	183
<i>R</i> <sub>work</sub> (%)	21.21 (32.68)
<i>R</i> <sub>free</sub> (%)	22.93 (31.57)
Average <i>B</i> factor for protein atoms (Å <sup>2</sup> )	84.09
R.m.s. deviations from ideality	
Bond lengths (Å)	0.01
Bond angles (°)	1.21
Ramachandran plot	
Favoured regions (%)	94
Allowed regions (%)	4.7
Outlier regions (%)	0.93

and *REFMAC* v.05.07.0029 (Winn *et al.*, 2011; Murshudov *et al.*, 2011), respectively. The quality of the structures was evaluated according to the wwPDB Validation Task Force (Read *et al.*, 2011). Topology was represented using the *PDBsum* server (Laskowski *et al.*, 1997; de Beer *et al.*, 2014). Molecular graphics were produced and analyses were performed with the *UCSF Chimera* package and *PyMOL* (Schrödinger). *UCSF Chimera* was developed by the Resource for Biocomputing, Visualization and Informatics at the University of California, San Francisco (supported by NIGMS P41-GM103311; Pettersen *et al.*, 2004). Secondary structure was confirmed using the *DSSP* server (Kabsch & Sander, 1983; Joosten *et al.*, 2011). The final structure was analyzed using the *Protein Interfaces, Surfaces and Assemblies (PISA)* server at the European Bioinformatics Institute ([http://www.ebi.ac.uk/pdbe/prot\\_int/pistart.html](http://www.ebi.ac.uk/pdbe/prot_int/pistart.html); Krissinel & Henrick, 2007).

### 3. Results and discussion

The XfsHSP17.9 structure is similar to those of other sHSPs, with a conserved structural organization: an N-terminal region followed by both the known ACD motif and a conserved C-terminal portion. It forms a compact  $\beta$ -sheet sandwich that consists of two layers of antiparallel  $\beta$ -sheets formed by seven  $\beta$ -strands ( $\beta$ <sub>2</sub>– $\beta$ <sub>9</sub>) connected by a long interdomain loop and an unfolded C-terminal portion (Fig. 1). Refinement statistics are summarized in Table 1.

The interdomain region is a loop that is involved in dimer formation; it usually links two  $\beta$ -strands, but in this case a <sub>310</sub>-helix (h2) follows the  $\beta$ <sub>5</sub> strand, thus connecting h2 and  $\beta$ <sub>6</sub>– $\beta$ <sub>7</sub>. The XfsHSP17.9 structure supports the results from previous circular-dichroism spectroscopy, which showed that the secondary structure of the protein is composed mainly of

$\beta$ -strands and a few short helices (Azzoni *et al.*, 2004). The motifs known to be conserved throughout the sHSPs, AxxGVL and the two-residue region LP (leucine/proline residues located upstream from the first motif), were observed (Laksanalamai & Robb, 2004). This region in the  $\alpha$ -crystallin domain is involved in multi-subunit assembly.

The N-terminal portion, which is known to be disordered, was not resolved owing to a lack of electron density, suggesting high flexibility. In fact, this region was also not built in many other available crystallographic structures such as those of *M. jannaschii* HSP16.5 (PDB entries 1shs and 4eld; Kim *et al.*, 1998; Mchaourab *et al.*, 2012), *R. norvegicus* HSP20 (PDB entry 2wj5; Bagn ris *et al.*, 2009), *S. cerevisiae* HSP26.0 (PDB entries 2h50 and 2h53; White *et al.*, 2006) and *X. citri* HspA (PDB entries 3gla and 3gt6; Hilario *et al.*, 2006, 2011). The exceptions are the *T. aestivum* HSP16.9 (PDB entry 1gme; van Montfort *et al.*, 2001) and *S. tokodaii* HSP14.0 (PDB entries 3aab and 3aac; Takeda *et al.*, 2011) structures, in which this region is partially resolved.

Furthermore, sHSPs have a conserved ACD motif. The ACD motif can dimerize through the formation of hydrogen bonds to the interdomain loop (the region near h2) from the molecule related by crystallographic symmetry, and this dimer is a building block that is required for the formation of the high-order structure (Figs. 2c and 2d).

One of the most notable properties of the sHSPs is their organization into large oligomeric structures (Laksanalamai & Robb, 2004). They often form a high-molecular-mass complex (between 150 and 800 kDa), even though some sHSPs occur as dimers or tetramers (Kapp  *et al.*, 2002). The C-terminal portion is involved in oligomer stabilization. Analysis of several sHSP structures revealed that this portion has the consensus sequence motif I-X-I/V and is a known interaction region in sHSPs (de Jong *et al.*, 1998). This moiety can dock into pockets on one side of a neighbouring ACD-motif sandwich, driving the formation of a high-order assembly.

In the present structure, contacts between Ile145 and Val147 (Fig. 2b) and the hydrophobic groove between  $\beta$ <sub>4</sub> and  $\beta$ <sub>8</sub> are important for high-order structure formation. Furthermore, the C-terminus contains polar amino acids (Arg, Asn and Gln) that can contribute to multi-unit assembly through hydrogen bonds to the same  $\beta$ -strands of the neighbouring molecule, thus helping with ‘inter-dimer’ interface stabilization. Thus, the dimers interact with each other linearly and laterally to form ‘meshes’ that intersect nearly orthogonally, as shown in Fig. 2(c). As a result, although the symmetry described in Fig. 2(c) is extracted from the space group, it could show elements of an assembly used to construct a particle of defined higher molecular weight.

Interestingly, the combination of dimers leads to the formation of nearly square cavities along the *c* axis, with sides measuring up to 42 Å, which have not been observed before in other sHSPs. In fact, other sHSPs have oligomeric structures containing a dodecameric double disc (*T. aestivum* HSP16.9; van Montfort *et al.*, 2001), a hollow sphere with a diameter of 120 Å containing 24 subunits (*M. jannaschii* HSP16.5; Kim *et al.*, 1998) and a spherical structure with a diameter of 115 Å

containing 24 subunits (*S. tokodaii* HSP14.0; Hanazono *et al.*, 2012) (Fig. 2a).

These differences, which are related to the ‘inter-dimer’ interaction, are mainly owing to the differences in the amino-acid residues of the C-terminus involved in these interactions. For example, XfsHSP17.9 and *T. aestivum* HSP16.9 have C-terminal sequences PKRAATTPRRIQVGN

and PKAEVKKPEVKAIQISG, respectively (starting from Pro135). A simple alignment reveals that there are different amino acids with different side-chain properties at the same positions in the sequences. The side chains are implicated in the specific kind of intermolecular interactions that occur. For example, the replacement of a threonine residue in the *X. fastidiosa* structure by a lysine in the *T. aestivum* structure

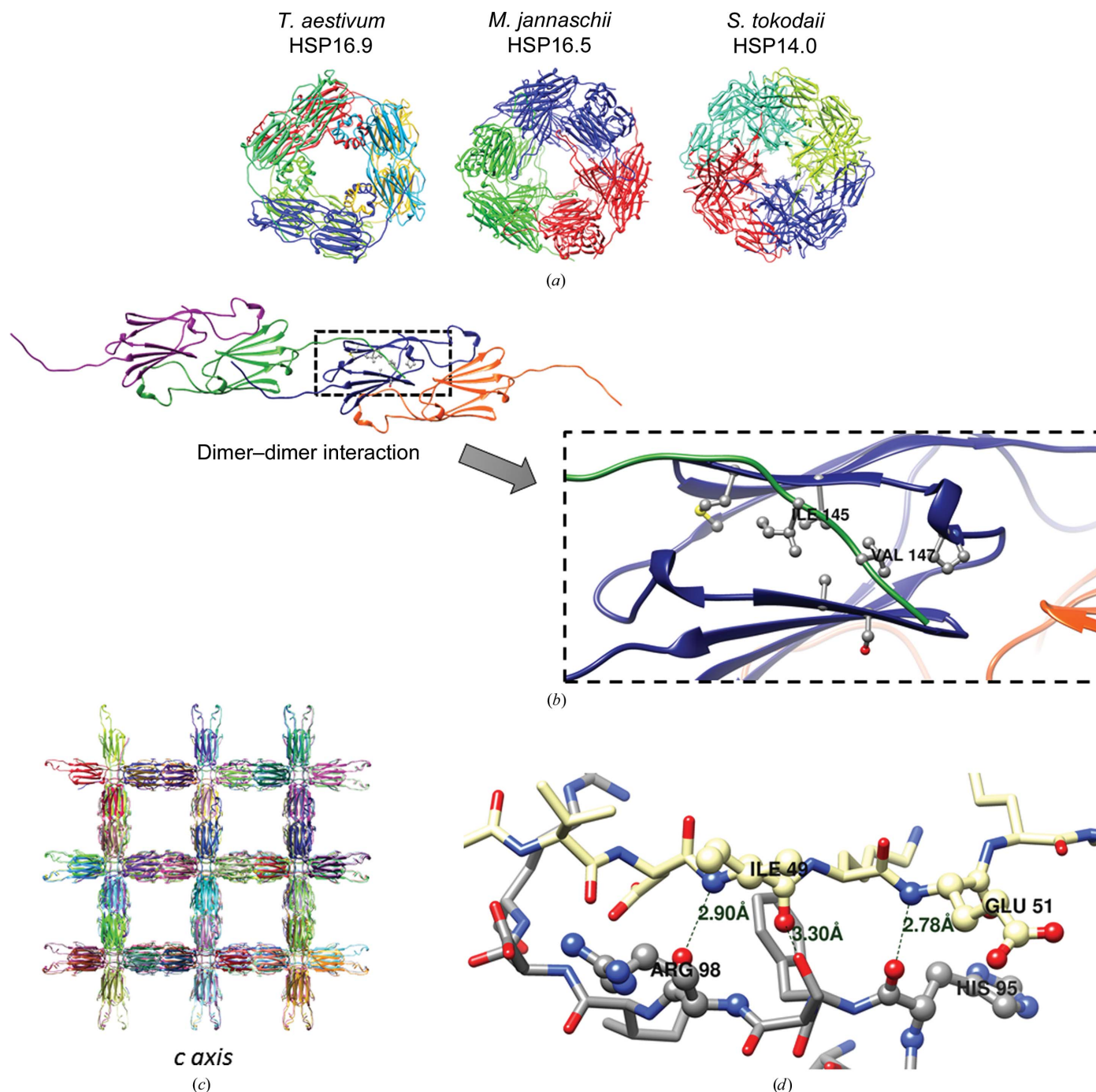


**Figure 2**  
 (a) Oligomeric structures of other sHSPs for comparison. (b) XfsHSP17.9 dimer–dimer assembly. The enlargement shows the surroundings of Ile145 and Val147. (c) High-order structure of XfsHSP17.9 viewed along the *c* axis. The formation of nearly square channels is observed along the crystallographic *c* axis. (d) Hydrogen bonds between the ACD motif and the interdomain loop (the region near helix h2) of the molecule related by crystallographic symmetry. The colours of the ribbons were assigned randomly in order to differentiate between neighbouring protein chains.

involves the change of a polar uncharged side chain to a positively electrically charged one (the residues shown in bold above).

In order to provide further insights into the interactions in the high-order structure of XfsHSP17.9, we conducted a computational evaluation using the PISA server. The inter-dimer interactions observed within the asymmetric unit cell involve 22 hydrogen bonds. The inter-unit-cell dimer interface, which is responsible for cavity formation, is held together by 34 hydrogen bonds and 20 salt bridges and has a larger contact area. This indicates that the interactions involved in the formation of the unusual cavity are stronger than those in the inter-dimer interface.

Further biochemical studies are required to verify the functional relevance of the observed arrangement, and the crystallographic structure reported here provides a starting point for such studies. As reported previously, despite several experiments aimed at determination of the molecular mass of the quaternary structure, analysis of the formation of oligomeric complexes of XfsHSP17.9 in solution was not conclusive. Thus, although the present structure reveals a novel high-order assembly, further functional studies are required in order to correlate its structure with the previously published chaperone-like activity (Azzoni *et al.*, 2004).

#### 4. Conclusions

In this work, we present the crystallographic structure of a small heat-shock protein from *X. fastidiosa*, the phytopathogenic organism that causes citrus variegated chlorosis. This 2.9 Å resolution structure reveals a distinct high-order assembly. The XfsHSP17.9 monomer forms dimers that interact with each other, composing a three-dimensional mesh. As a result, a nearly square cavity is formed.

#### Acknowledgements

This study was supported by grants from the São Paulo Research Foundation (FAPESP; grants Nos. 2008/52197-4 and 2001/07533-7). SFST, CAS and MAST received fellowships from FAPESP (2002/01316-7 PD, 2008/55690-3 DR and 2006/52844-4 IC). APS is the recipient of a research fellowship from the Conselho Nacional de Desenvolvimento Científico e Tecnológico (CNPq).

#### Funding information

Funding for this research was provided by: Fundação de Amparo à Pesquisa do Estado de São Paulo (award Nos. 2008/52197-4, 2001/07533-7, 2002/01316-7, 2008/55690-3, 2006/52844-4).

#### References

Allen, S. P., Polazzi, J. O., Gierse, J. K. & Easton, A. M. (1992). *J. Bacteriol.* **174**, 6938–6947.  
 Azzoni, A. R., Tada, S. F. S., Rosselli, L. K., Paula, D. P., Catani, C. F., Sabino, A. A., Barbosa, J. A. R. G., Guimarães, B. G., Eberlin,

M. N., Medrano, F. J. & Souza, A. P. (2004). *Protein Expr. Purif.* **33**, 297–303.  
 Bagnéris, C., Bateman, O. A., Naylor, C. E., Cronin, N., Boelens, W. C., Keep, N. H. & Slingsby, C. (2009). *J. Mol. Biol.* **392**, 1242–1252.  
 Beer, T. A. P. de, Berka, K., Thornton, J. M. & Laskowski, R. A. (2014). *Nucleic Acids Res.* **42**, D292–D296.  
 Bepperling, A., Alte, F., Kriehuber, T., Braun, N., Weinkauff, S., Groll, M., Haslbeck, M. & Buchner, J. (2012). *Proc. Natl Acad. Sci. USA*, **109**, 20407–20412.  
 Bova, M. P., Mchaourab, H. S., Han, Y. & Fung, B. K.-K. (2000). *J. Biol. Chem.* **275**, 1035–1042.  
 Emsley, P. & Cowtan, K. (2004). *Acta Cryst.* **D60**, 2126–2132.  
 Fleckenstein, T., Kastenmüller, A., Stein, M. L., Peters, C., Daake, M., Krause, M., Weinfurtnner, D., Haslbeck, M., Weinkauff, S., Groll, M. & Buchner, J. (2015). *Mol. Cell*, **58**, 1067–1078.  
 Hanazono, Y., Takeda, K., Oka, T., Abe, T., Tomonari, T., Akiyama, N., Aikawa, Y., Yohda, M. & Miki, K. (2013). *Structure*, **21**, 220–228.  
 Hanazono, Y., Takeda, K., Yohda, M. & Miki, K. (2012). *J. Mol. Biol.* **422**, 100–108.  
 Haslbeck, M., Franzmann, T., Weinfurtnner, D. & Buchner, J. (2005). *Nature Struct. Mol. Biol.* **12**, 842–846.  
 Haslbeck, M., Walke, S., Stromer, T., Ehrnsperger, M., White, H. E., Chen, S., Saibil, H. R. & Buchner, J. (1999). *EMBO J.* **18**, 6744–6751.  
 Hilario, E., Martin, F. J. M., Bertolini, M. C. & Fan, L. (2011). *J. Mol. Biol.* **408**, 74–86.  
 Hilario, E., Teixeira, E. C., Pedroso, G. A., Bertolini, M. C. & Medrano, F. J. (2006). *Acta Cryst.* **F62**, 446–448.  
 Horwitz, J. (1992). *Proc. Natl Acad. Sci. USA*, **89**, 10449–10453.  
 Jakob, U., Gaestel, M., Engel, K. & Buchner, J. (1993). *J. Biol. Chem.* **268**, 1517–1520.  
 Jong, W. W. de, Caspers, G. J. & Leunissen, J. A. M. (1998). *Int. J. Biol. Macromol.* **22**, 151–162.  
 Joosten, R. P., te Beek, T. A. H., Krieger, E., Hekkelman, M. L., Hooft, R. W. W., Schneider, R., Sander, C. & Vriend, G. (2011). *Nucleic Acids Res.* **39**, D411–D419.  
 Kabsch, W. & Sander, C. (1983). *Biopolymers*, **22**, 2577–2637.  
 Kappé, G., Leunissen, J. A. & de Jong, W. W. (2002). *Prog. Mol. Subcell. Biol.* **28**, 1–17.  
 Kim, K. K., Kim, R. & Kim, S.-H. (1998). *Nature (London)*, **394**, 595–599.  
 Krissinel, E. & Henrick, K. (2007). *J. Mol. Biol.* **372**, 774–797.  
 Laksanalamai, P. & Robb, F. T. (2004). *Extremophiles*, **8**, 1–11.  
 Laskowski, R. A., Hutchinson, E. G., Michie, A. D., Wallace, A. C., Jones, M. L. & Thornton, J. M. (1997). *Trends Biochem. Sci.* **22**, 488–490.  
 Lee, G. J., Roseman, A. M., Saibil, H. R. & Vierling, E. (1997). *EMBO J.* **16**, 659–671.  
 Mchaourab, H. S., Lin, Y.-L. & Spiller, B. W. (2012). *Biochemistry*, **51**, 5105–5112.  
 Montfort, R. L. M. van, Basha, E., Friedrich, K. L., Slingsby, C. & Vierling, E. (2001). *Nature Struct. Biol.* **8**, 1025–1030.  
 Murshudov, G. N., Skubák, P., Lebedev, A. A., Pannu, N. S., Steiner, R. A., Nicholls, R. A., Winn, M. D., Long, F. & Vagin, A. A. (2011). *Acta Cryst.* **D67**, 355–367.  
 Oetelaar, P. J. M. van den, van Someren, P. F., Thomson, J. A., Siezen, R. J. & Hoenders, H. J. (1990). *Biochemistry*, **29**, 3488–3493.  
 Pettersen, E. F., Goddard, T. D., Huang, C. C., Couch, G. S., Greenblatt, D. M., Meng, E. C. & Ferrin, T. E. (2004). *J. Comput. Chem.* **25**, 1605–1612.  
 Rao, C. M., Raman, B., Ramakrishna, T., Rajaraman, K., Ghosh, D., Datta, S., Trivedi, V. D. & Sukhaswami, M. B. (1998). *Int. J. Biol. Macromol.* **22**, 271–281.  
 Read, R. J. *et al.* (2011). *Structure*, **19**, 1395–1412.  
 Rossetti, V., Garnier, M., Bove, J. M., Beretta, M. J. G., Teixeira, A. R. R., Quaggio, J. A. & De Negri, J. D. (1990). *C. R. Acad. Sci. Ser. III*, **310**, 345–349.

- Saibil, H. (2000). *Curr. Opin. Struct. Biol.* **10**, 251–258.
- Shashidharamurthy, R., Koteiche, H. A., Dong, J. & Mchaourab, H. S. (2005). *J. Biol. Chem.* **280**, 5281–5289.
- Simpson, A. J. G. *et al.* (2000). *Nature (London)*, **406**, 151–157.
- Slepenkov, S. V. & Witt, S. N. (2002). *Mol. Microbiol.* **45**, 1197–1206.
- Stamler, R., Kappé, G., Boelens, W. & Slingsby, C. (2005). *J. Mol. Biol.* **353**, 68–79.
- Tada, S. F. S., Saraiva, A. M., Lorite, G. S., Rosselli-Murai, L. K., Pelloso, A. C., dos Santos, M. L., Trivella, D. B. B., Cotta, M. A., de Souza, A. P. & Aparicio, R. (2012). *Acta Cryst.* **F68**, 535–539.
- Takeda, K., Hayashi, T., Abe, T., Hirano, Y., Hanazono, Y., Yohda, M. & Miki, K. (2011). *J. Struct. Biol.* **174**, 92–99.
- Trent, J. D. (1996). *FEMS Microbiol. Rev.* **18**, 249–258.
- Waters, E. R., Lee, G. J. & Vierling, E. (1996). *J. Exp. Bot.* **47**, 325–338.
- White, H. E., Orlova, E. V., Chen, S., Wang, L., Ignatiou, A., Gowen, B., Stromer, T., Franzmann, T. M., Haslbeck, M., Buchner, J. & Saibil, H. R. (2006). *Structure*, **14**, 1197–1204.
- Winn, M. D. *et al.* (2011). *Acta Cryst.* **D67**, 235–242.
- Yang, H., Huang, S., Dai, H., Gong, Y., Zheng, C. & Chang, Z. (1999). *Protein Sci.* **8**, 174–179.